PERGAMON

International Journal of Heat and Mass Transfer 45 (2002) 417–424

International Journal of HEAT and MASS TRANSFER

www.elsevier.com/locate/ijhmt

Internal distribution of radiation absorption in one-dimensional semitransparent medium

L.H. Liu *, H.P. Tan, Q.Z. Yu

School of Energy Science and Engineering, Harbin Institute of Technology, 92 West Dazhi Street, Harbin 150001, People's Republic of China

Received 8 February 2001

Abstract

The internal distribution of spectral radiation absorption in one-dimensional semitransparent slab, sphere and cylinder irradiated uniformly and isotropically is determined by the ray tracing method, and the detailed theory for computation are deduced. The computed results show that the internal distribution of spectral radiation absorption in slab differs from that in spherical and cylindrical particles. The peak of internal volumetric spectral radiation absorption may locate at interior shell of the semitransparent sphere and cylinder. The dimensionless volumetric spectral radiation absorption is higher near the center for weakly absorbing or small size parameter, but is higher near the surface for strongly absorbing or large spheres and cylinders. Refraction focuses the rays close to the sphere and cylinder center. With the increases of the refractive index, the dimensionless volumetric spectral radiation absorption increases near the sphere and cylinder centers and decreases near the sphere and cylinder surfaces. © 2001 Elsevier Science Ltd. All rights reserved.

Keywords: Semitransparent slab; Semitransparent sphere; Semitransparent cylinder; Radiant absorption; Ray tracing method

1. Introduction

Temperature distributions within semitransparent materials can be strongly affected by internal emission, scattering and absorption of radiant thermal energy. This is important for translucent materials at elevated temperatures, in high temperature surroundings or with large incident radiation. It is well known that local absorption of the radiation by a semitransparent medium is generally nonuniform over its volume. Knowledge of the local distribution of absorbed radiation energy within a semitransparent medium is essential for the improvement of the performance of some industrial processes, for example, spray combustion, infrared heating and drying.

Recently, much attention has been focused by many researchers on the transient heat transfer in semitransparent materials. Siegel [1] gave the detailed review of the literatures surrounding the subject over the past 40 years and pointed out that the key difficulty for the solution of transient heat transfer is the determination of the local radiant source term in energy equation. Despite the relatively large interest expressed in the theoretical solution of radiant absorption in semitransparent medium, most of the work has considered the slab geometrical systems. Only a limited amount of work is available on the theoretical solution of the radiant source term in semitransparent spherical geometrical systems. Tuntomo [2] and Lage [3] applied electromagnetic theory to study the internal radiant absorption field of a small spherical particle. Based on the electromagnetic theory, Mackowski et al. [4] presented series expressions for the radial-dependent absorption cross-section and heat source function in a stratified sphere. Dombrovsky [5] used Mie theory and a new differential approximation for radiation transfer to determine the radial profile of the radiation heat source inside an isothermal particle. Generally, the scattering and absorption of radiation by semitransparent medium can be

* Corresponding author. Tel.: +86-451-6414315; fax: +86-451-622-1048.

E-mail address: liulh_hit@263.net (L.H. Liu).

0017-9310/02/$ - see front matter © 2001 Elsevier Science Ltd. All rights reserved.
PII: S0017-9310(01)00142-9

Nomenclature

$h(y)$	local volumetric radiation absorption of surroundings irradiation
h_{av}	average volumetric radiation absorption of surroundings irradiation
m	complex index of refraction $m = n - i\kappa$,
n	refractive index
I_s	spectral radiative intensity of the incident ray from the surroundings
$I_{\perp,0}$	perpendicular polarized components of radiative intensity
$I_{\parallel,0}$	parallel polarized components of radiative intensity
$Q(y)$	radiant absorption defined in Eqs. (12), (13) and (15)
R	half thickness of slab, radius of sphere and cylinder
r	coordinate shown in Figs. 1–3
x	size parameter $x = 2\pi R/\lambda$,
y	dimensionless coordinate $y = r/R$,

Greek symbols

θ	incident angle
κ	extinction coefficient
λ	wavelength in vacuum
ξ	local dimensionless volumetric radiant absorption, $\xi = h(y)/h_{av}$
$\rho_\perp$	perpendicular polarized component of spectral reflectivity
$\rho_\parallel$	parallel polarized component of spectral reflectivity
ϕ	initial refraction angle, incident angle for internal reflection
ω	azimuthal angle

handled by electromagnetic theory or Mie theory. However, the computation by electromagnetic theory or Mie theory is complex and time-consuming. Mie's theory can be approximated with ray optics when the characteristic size of system is much larger than the wavelength.

The objective of the present work is to study the local volumetric spectral radiation absorption within one-dimensional semitransparent slab, sphere and cylinder irradiated uniformly and isotropically by the ray tracing method and to deduce the detailed theoretical computation formulae for the internal spectral radiation absorption of these one-dimensional geometrical systems. The effects of the related parameters on the internal distribution of spectral radiation absorption for different one-dimensional geometrical systems will be analyzed and discussed.

2. Physical model and formulation

We consider one-dimensional semitransparent slab, sphere and cylinder surrounded by nonattenuating medium with unit index of refraction. These geometrical systems are irradiated uniformly and isotropically from the surroundings. The slab, sphere and cylinder are assumed to be composed of isotropic and homogeneous medium with complex index of refraction $m = n - i\kappa$, and the media constructed these geometrical systems absorb but do not scatter thermal radiation. In addition, the boundaries are assumed to be optically smooth.

The physical geometry of an infinite semitransparent slab with thickness $2R$ is shown in Fig. 1. Considering a ray irradiating the slab with incident angle θ from the surroundings, the refraction angle ϕ is related to the incident angle and the refractive index through Snell's law as

$$\sin\phi = \frac{1}{n}\sin\theta. \tag{1}$$

The reflectance of external specular reflection can be expressed as [6]:

$$\rho_\perp(\theta) = \frac{(\cos\theta - u)^2 + v^2}{(\cos\theta + u)^2 + v^2}, \tag{2a}$$

$$\rho_\parallel(\theta) = \frac{\left(u\cos\theta - \sin^2\theta\right)^2 + v^2\cos^2\theta}{\left(u\cos\theta + \sin^2\theta\right)^2 + v^2\cos^2\theta}\rho_\perp(\theta), \tag{2b}$$

where $\rho_\perp$ and $\rho_\parallel$ are perpendicular and parallel polarized components, respectively, u and v are the coefficients given by:

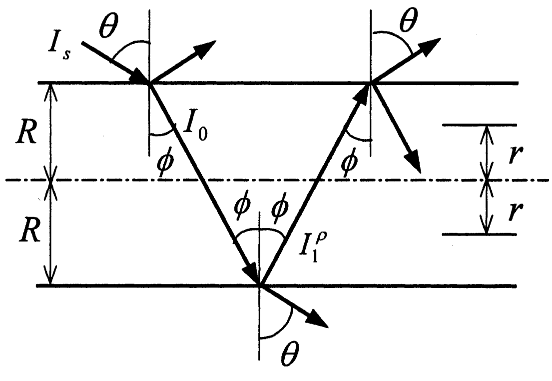

Fig. 1. Physical geometry of the semitransparent slab and ray tracing.

$$u^2 = 0.5\left\{\left[\left(n^2-\kappa^2-\sin^2\theta\right)^2+4n^2\kappa^2\right]^{0.5} + \left(n^2-\kappa^2-\sin^2\theta\right)\right\}, \quad (3a)$$

$$v^2 = 0.5\left\{\left[\left(n^2-\kappa^2-\sin^2\theta\right)^2+4n^2\kappa^2\right]^{0.5} - \left(n^2-\kappa^2-\sin^2\theta\right)\right\}. \quad (3b)$$

In order to derive the computational formulae of internal radiation absorption of the slab, let us trace an incident ray from the surroundings with an incidence angle θ. The ray enters the slab with the initial refraction angle ϕ. After entering the slab, the ray will undergo multiple reflection and refraction. By symmetry, ϕ becomes the incident angle for all internal reflections, and $2R/\cos\phi$ is the distance travelled between consecutive surface encounters. The reflectances of internal specular reflection are equal to that of external specular reflection if expressed in term of the angle θ. For the unpolarized incident radiation from the surroundings, the relation between the radiative intensities of the initial incident and refracted rays can be determined by energy equilibrium as:

$$I_{\perp,0} = 0.5[1-\rho_\perp(\theta)]I_{\mathrm{s}}\frac{\sin\theta\cos\theta\,\mathrm{d}\theta}{\sin\phi\cos\phi\,\mathrm{d}\phi}, \quad (4a)$$

$$I_{\parallel,0} = 0.5\left[1-\rho_\parallel(\theta)\right]I_{\mathrm{s}}\frac{\sin\theta\cos\theta\,\mathrm{d}\theta}{\sin\phi\cos\phi\,\mathrm{d}\phi}, \quad (4b)$$

where I_{s} is the spectral radiative intensity of the incident ray, $I_{\perp,0}$ and $I_{\parallel,0}$ are the perpendicular and parallel polarized components of radiative intensity of the initial refracted ray, respectively. For perpendicular component, after the first internal reflection, radiative intensity of the reflected ray becomes as

$$I^{\rho}_{\perp,1} = I_{\perp,0}\rho_\perp(\theta)\exp\left[-\left(\frac{4\pi\kappa}{\lambda}\right)\frac{2R}{\cos\phi}\right] = I_{\perp,0}\rho_\perp(\theta)\exp\left(-\frac{4x\kappa}{\cos\phi}\right), \quad (5)$$

where x is the size parameter of slab defined as

$$x = \frac{2\pi R}{\lambda}. \quad (6)$$

After the kth internal reflection, the perpendicular radiative intensity component of the reflected ray is given as:

$$I^{\rho}_{\perp,k} = I_{\perp,0}[\rho_\perp(\theta)\exp(-4x\kappa/\cos\phi)]^k. \quad (7)$$

During the kth and $(k+1)$th reflection, the perpendicular radiative intensity component absorbed by the slab with thickness $2r$ can be written as

$$\Delta I^{\mathrm{a}}_{\perp,k} = I_{\perp,0}\left[\rho_\perp(\theta)\exp\left(-\frac{4x\kappa}{\cos\phi}\right)\right]^k \times\left\{\exp\left[-\frac{2x\kappa(1-y)}{\cos\phi}\right]-\exp\left[-\frac{2x\kappa(1+y)}{\cos\phi}\right]\right\}, \quad (8)$$

where y is the dimensionless thickness defined as

$$y = \frac{r}{R}. \quad (9)$$

The absorption of the perpendicular radiative intensity component in the infinite series of internal reflection traversals of a single ray can be summed as

$$\Delta I^{\mathrm{a}}_{\perp} = \sum_{k=0}^{\infty}\Delta I^{\mathrm{a}}_{\perp,k} = I_{\perp,0}\left\{\exp\left[-\frac{2x\kappa(1-y)}{\cos\phi}\right] - \exp\left[-\frac{2x\kappa(1+y)}{\cos\phi}\right]\right\} \times\left[1-\rho_\perp(\theta)\exp\left(-\frac{4x\kappa}{\cos\phi}\right)\right]^{-1}. \quad (10)$$

Similarly, the absorption of the parallel radiative intensity component in the infinite series of internal reflection traversals of a single ray can be written as

$$\Delta I^{\mathrm{a}}_{\parallel} = \sum_{k=0}^{\infty}\Delta I^{\mathrm{a}}_{\parallel,k} = I_{\parallel,0}\left\{\exp\left[-\frac{2x\kappa(1-y)}{\cos\phi}\right] - \exp\left[-\frac{2x\kappa(1+y)}{\cos\phi}\right]\right\} \times\left[1-\rho_\parallel(\theta)\exp\left(-\frac{4x\kappa}{\cos\phi}\right)\right]^{-1}. \quad (11)$$

After integration over the range of solid angle, considering the symmetry, we can derive the following relation for spectral radiation absorption per unit area of a slab with dimensionless thickness $2y$:

$$Q(y) = 2\pi I_{\mathrm{s}}\int_0^{\frac{\pi}{2}}\{\exp[-2x\kappa(1-y)/\cos\phi] - \exp[-2x\kappa(1+y)/\cos\phi]\} \times\left\{\frac{[1-\rho_\perp(\theta)]}{[1-\rho_\perp(\theta)\exp(-4x\kappa/\cos\phi)]} + \frac{[1-\rho_\parallel(\theta)]}{\left[1-\rho_\parallel(\theta)\exp(-4x\kappa/\cos\phi)\right]}\right\}\sin\theta\cos\theta\,\mathrm{d}\theta. \quad (12)$$

The physical geometry of a semitransparent sphere with radius R is shown in Fig. 2. Similarly to the

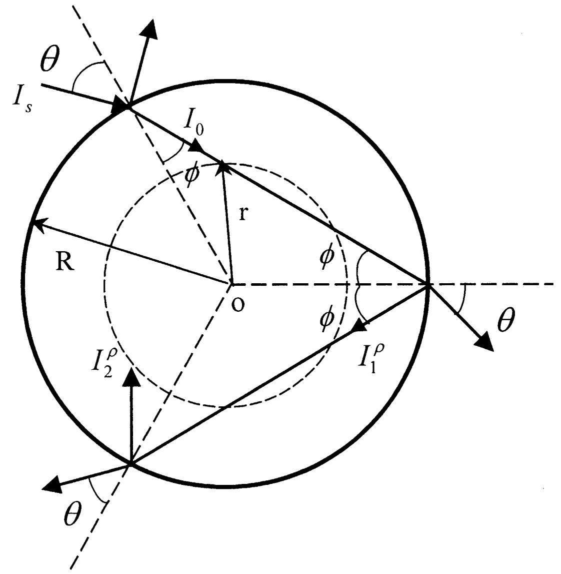

Fig. 2. Physical geometry of the semitransparent sphere and ray tracing.

semitransparent slab, the spectral radiation absorption of the sphere with dimensionless radius y can be written as

$$Q(y) = 4\pi^2 R^2 I_s \int_0^{\theta_{\mathrm{end}}} \left\{ \exp\left[-2x\kappa\left(\cos\phi - \sqrt{y^2 - \sin^2\phi} \right)\right] - \exp\left[-2x\kappa\left(\cos\phi + \sqrt{y^2 - \sin^2\phi} \right)\right] \right\} \times \left\{ \frac{[1-\rho_\perp(\theta)]}{[1-\rho_\perp(\theta)\exp(-4x\kappa\cos\phi)]} + \frac{[1-\rho_\parallel(\theta)]}{\left[1-\rho_\parallel(\theta)\exp(-4x\kappa\cos\phi)\right]} \right\} \sin\theta\cos\theta\,\mathrm{d}\theta. \tag{13}$$

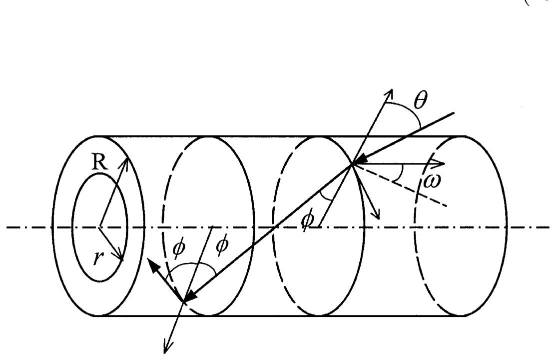

Fig. 3. Physical geometry of the semitransparent cylinder and ray tracing.

Here, θ_{end} is determined as following:

$$\theta_{\mathrm{end}} = 0.5\pi \quad \text{if } \frac{1}{n} < y \leqslant 1, \tag{14a}$$

$$\theta_{\mathrm{end}} = \sin^{-1}(ny) \quad \text{if } 0 \leqslant y \leqslant \frac{1}{n}. \tag{14b}$$

The physical geometry of a semitransparent cylinder with radius R is shown in Fig. 3. Similarly to the semitransparent slab and sphere, the spectral radiation absorption per unit axial length of the cylinder with dimensionless radius y can be expressed as

$$Q(y) = \pi R I_s \times \int_0^{\theta_{\mathrm{end}}(\omega)} \int_0^{2\pi} \left\{ \exp\left[-2x\kappa\left(\frac{\cos\phi}{\cos^2\phi + \sin^2\phi\sin^2\omega} - \frac{\sqrt{y^2 - 1 + \alpha^2}}{\sqrt{\cos^2\phi + \sin^2\phi\sin^2\omega}} \right)\right] - \exp\left[-2x\kappa\left(\frac{\cos\phi}{\cos^2\phi + \sin^2\phi\sin^2\omega} + \frac{\sqrt{y^2 - 1 + \alpha^2}}{\sqrt{\cos^2\phi + \sin^2\phi\sin^2\omega}} \right)\right] \right\} \times \left\{ \left[\{1-\rho_\perp(\theta)\} \Big/ \left\{ 1-\rho_\perp(\theta) \times \exp\left(-\left(\frac{4x\kappa\cos\phi}{\cos^2\phi + \sin^2\phi\sin^2\omega} \right)\right) \right\} \right] + \left[\{1-\rho_\parallel(\theta)\} \Big/ \left\{ 1-\rho_\parallel(\theta) \times \exp\left(-\left(\frac{4x\kappa\cos\phi}{\cos^2\phi + \sin^2\phi\sin^2\omega} \right)\right) \right\} \right] \right\} \times \sin\theta\cos\theta\,\mathrm{d}\omega\,\mathrm{d}\theta, \tag{15}$$

where the parameter α is given by

$$\alpha = \frac{\cos\phi}{\sqrt{\cos^2\phi + \sin^2\phi\sin^2\omega}}, \tag{16}$$

and $\theta_{\mathrm{end}}(\omega)$ is determined by following function relation for any given azimuthal angle ω as

$$\max_{\theta_{\mathrm{end}}} \left\{ \frac{|\sin\theta_{\mathrm{end}}\sin\omega|}{\sqrt{n^2 - \sin^2\theta_{\mathrm{end}}(1-\sin^2\omega)}} \right\} \leqslant y. \tag{17}$$

The local and the average volumetric radiation absorption of surroundings irradiation, $h(y)$ and h_{av}, can be defined as

$$h(y) = \begin{cases} \dfrac{dQ(y)}{2dr} & \text{for slab,} \\ \dfrac{dQ(y)}{4\pi r^2 dr} & \text{for sphere,} \\ \dfrac{dQ(y)}{2\pi r dr} & \text{for cylinder,} \end{cases} \quad (18)$$

$$h_{av} = \begin{cases} \dfrac{Q(1)}{2R} & \text{for slab,} \\ \dfrac{3Q(1)}{4\pi R^3} & \text{for sphere,} \\ \dfrac{Q(1)}{\pi R^2} & \text{for cylinder.} \end{cases} \quad (19)$$

For the sake of comparison, the local dimensionless volumetric radiation absorption is expressed as

$$\xi(y) = \frac{h(y)}{h_{av}} \quad (20)$$

Eqs. (12), (13), (15) and (20) give the distribution profiles of internal radiation absorption inside the semitransparent slab, sphere and cylinder.

3. Results and discussion

Because the geometrical optics can approximate Mie theory well only if the characteristic size of system is larger than the wavelength of incident rays, we only consider here the internal distribution of spectral radiation absorption in the one-dimensional geometrical systems with size parameter $x \geqslant 30$. From Eqs. (12), (13) and Eq. (15), we can see that the size parameter and the complex index of refraction will affect the radial distribution profiles of internal spectral radiation absorption inside the semitransparent slab, sphere and cylinder.

Fig. 4 shows the dimensionless internal spectral absorption distribution within semitransparent slab for four different size parameters, from which we can find the internal volumetric spectral absorption of semitransparent slab is not uniform. With the increase of size parameter, the volumetric spectral absorption within semitransparent slab become more and more nonuniform. The volumetric spectral absorption in the site closed to the slab center decreases with the increase of the size parameter, but the volumetric spectral absorption in the site closed to the slab surface increases with the increase of the size parameter. From Eqs. (12) and (18), the deriviate $dh(y)/dy$ for semitransparent slab can be written as

$$\frac{dh(y)}{dy} = \frac{\pi I_s}{R} \int_0^{\frac{\pi}{2}} \{ \exp[-2x\kappa(1-y)/\cos\phi] - \exp[-2x\kappa(1+y)/\cos\phi] \} \left(\frac{2x\kappa}{\cos\phi} \right)^2 \times \left\{ \frac{[1-\rho_\perp(\theta)]}{[1-\rho_\perp(\theta)\exp(-4x\kappa/\cos\phi)]} + \frac{[1-\rho_\parallel(\theta)]}{\left[1-\rho_\parallel(\theta)\exp(-4x\kappa/\cos\phi)\right]} \right\} \sin\theta\cos\theta d\theta. \quad (21)$$

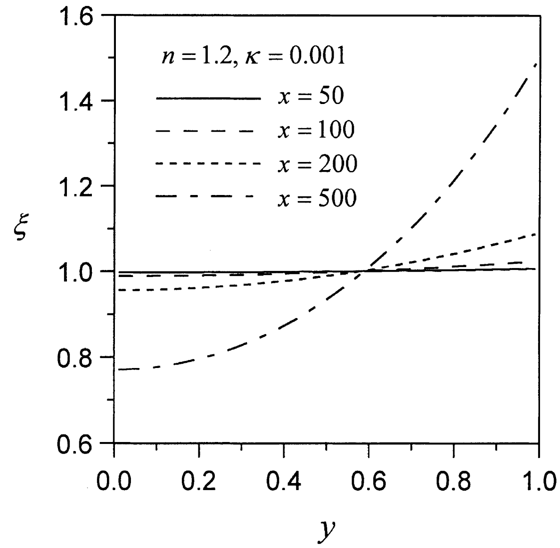

Fig. 4. The influences of the size parameter on the dimensionless internal spectral radiation absorption distribution within semitransparent slab.

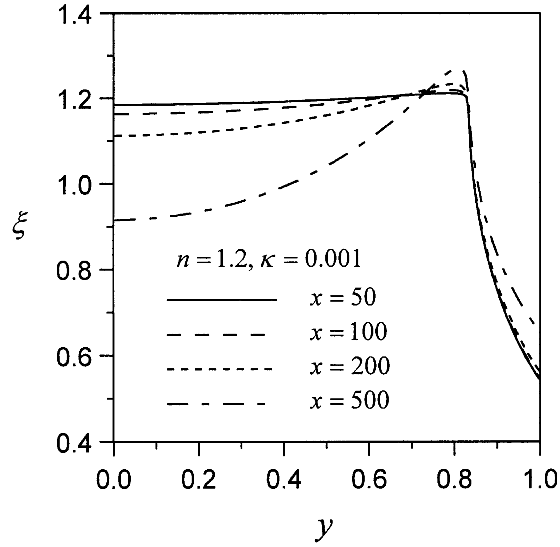

Fig. 5. The influences of the size parameter on the dimensionless internal spectral radiation absorption distribution within semitransparent sphere.

We can see from Eq. (21) that, $\mathrm{d}h(y)/\mathrm{d}y \geqslant 0$ for any y ($0 \leqslant y \leqslant 1$) and $h(y)$ is the monotonic function of y. The volumetric spectral absorption in the site closed to the slab center is always less than that in the site close to the slab surface.

The dimensionless radial internal spectral absorption distributions within semitransparent sphere and cylinder for four different size parameters are shown in Figs. 5 and 6, respectively. It can be seen that the peak of internal volumetric spectral absorption may locate at interior shell of the sphere and cylinder. This differs from the semitransparent slab, in which the maximum of radiant absorption always locates in the boundary of slab. The volumetric spectral absorption in the site closed to the sphere and cylinder centers decreases with the increase of the size parameter, but the volumetric spectral absorption in the site closed to the sphere and cylinder surfaces increases with the increase of the size parameter. The phenomena, in which the peak of internal volumetric spectral absorption locates at interior shell, may be related to the secondary atomization of droplet and the internal burst or overheating of spherical and cylindrical particles.

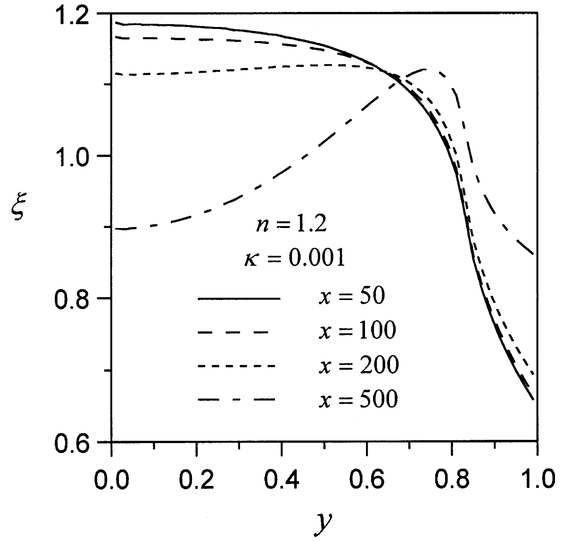

Fig. 6. The influences of the size parameter on the dimensionless internal spectral radiation absorption distribution within semitransparent cylinder.

The effects of the complex index of refraction on the internal spectral radiation absorption within semitransparent slab, sphere and cylinder are shown in Figs. 7–9, respectively. Due to the effects of Bear's law, the dimensionless volumetric spectral radiation absorption decreases with increasing of the extinction coefficient, κ, near the center and increases near the boundaries.

By comparison of Figs. 4–9, it can be seen that the dimensionless volumetric spectral radiation absorption is higher near the center for weakly absorbing or small size parameter, but is higher near the boundary for strongly absorbing or large spheres and cylinders. Since the refraction focuses the rays close to the sphere and cylinder center, the dimensionless volumetric spectral radiation absorption increases with increasing refractive index, n, near the center and decreases with increasing refractive index, n, near surfaces of semitransparent sphere and cylinder.

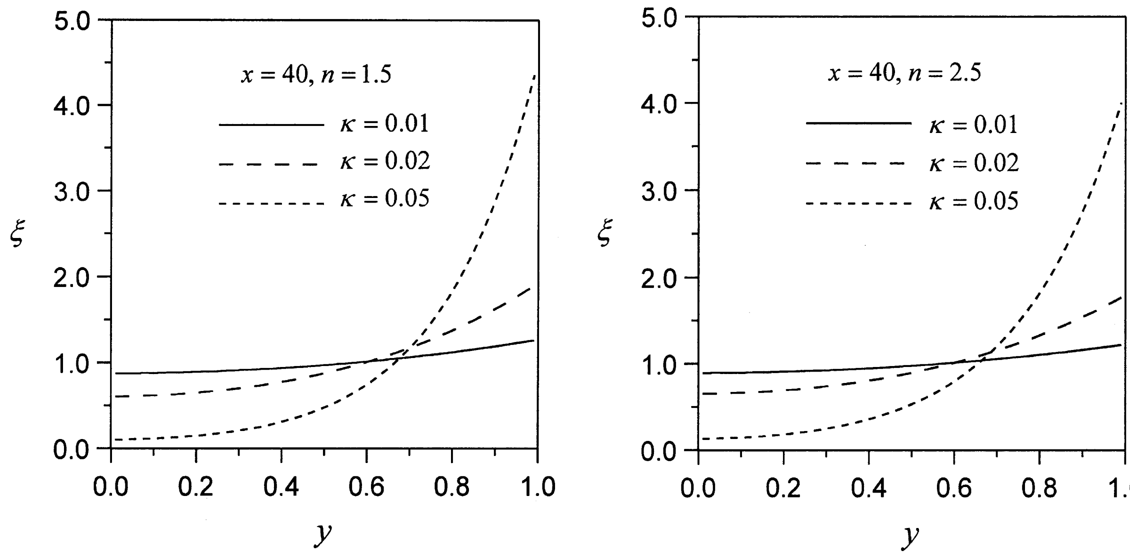

Fig. 7. The effects of the complex index of refraction on the dimensionless internal spectral radiation absorption distribution within semitransparent slab.

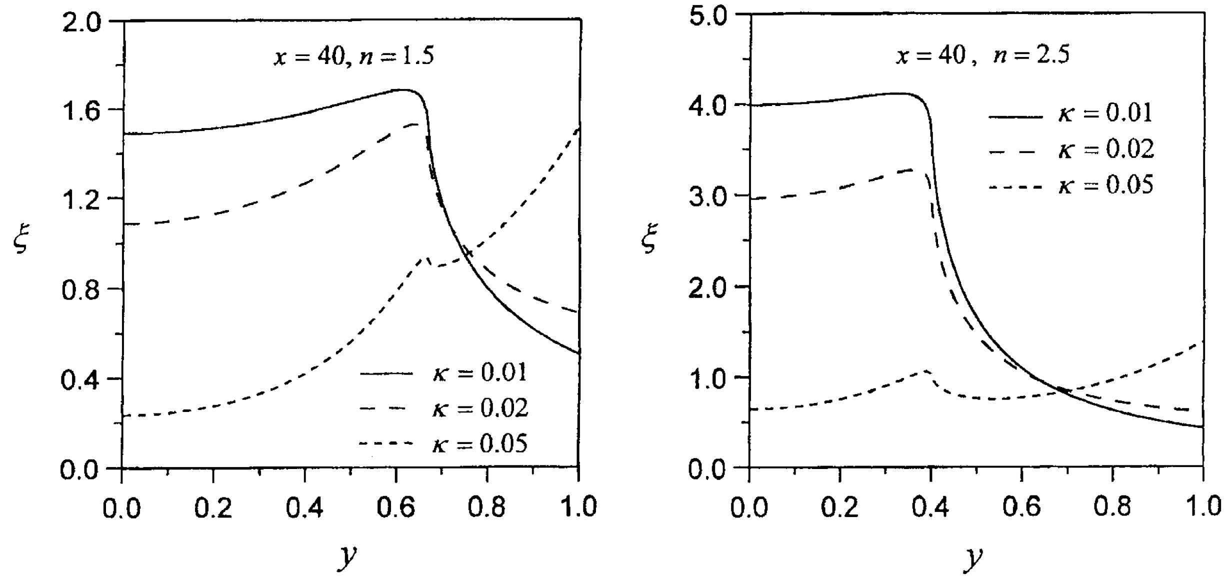

Fig. 8. The effects of the complex index of refraction on the dimensionless internal spectral radiation absorption distribution within semitransparent sphere.

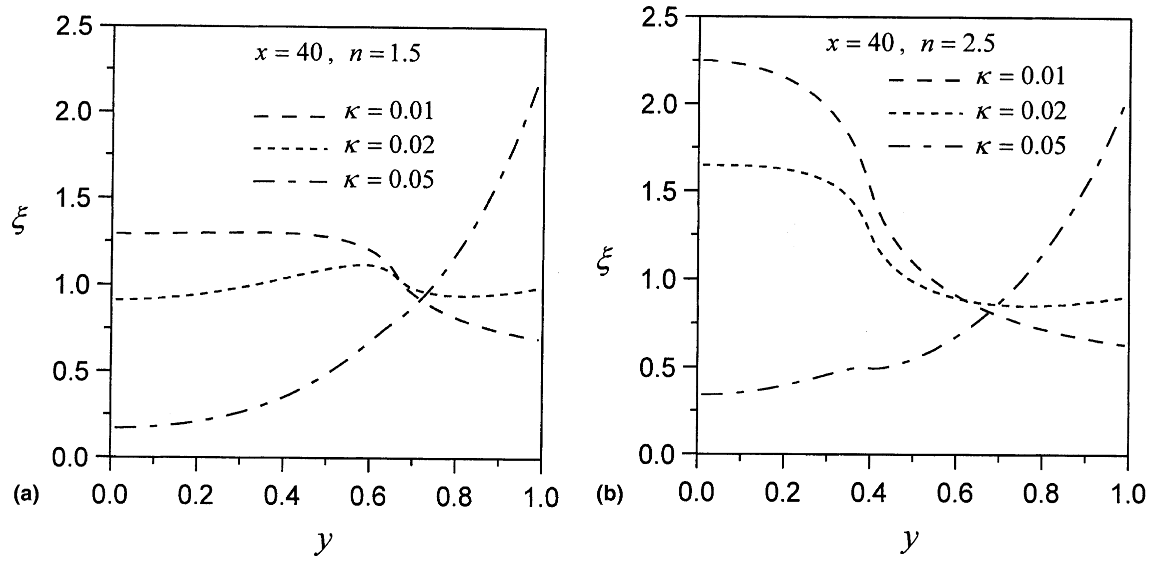

Fig. 9. The effects of the complex index of refraction on the dimensionless internal spectral radiation absorption distribution within semitransparent cylinder.

4. Conclusions

The main conclusions from the present analysis can be summarized as follows:

1. The internal volumetric spectral absorption of semitransparent slab is not uniform. The volumetric spectral absorption in the site close to the slab center is always less than that in the site close to the slab surface.
2. The peak of internal volumetric spectral radiation absorption may locate at interior shell of the semitransparent sphere and cylinder, especially in the cases of small extinction coefficient, large refractive index and small size parameter. This may be related to

the secondary atomization of droplet and the internal burst or overheating of spherical and cylindrical particles.

3. Refraction focuses the rays close to the sphere and cylinder center, the dimensionless volumetric spectral radiation absorption increases near the center and decreases near boundaries of sphere and cylinder with increasing of the refractive index, *n*.
4. For one-dimensional semitransparent sphere and cylinder, the dimensionless volumetric spectral radiation absorption is higher near the center for weakly absorbing or small size parameter, but is higher near the surface for strongly absorbing or larger spheres and cylinders.

Acknowledgements

The supports of this work by Fok Ying Tung Education Foundation (No. 71053), National Natural Science Foundation of China (No. 59706008), and the Scientific Research Foundation of Harbin Institute of Technology (Project No. HIT200072) are gratefully acknowledged.

References

[1] R. Siegel, Transient effects of radiative transfer in semitransparent materials, Int. J. Eng. Sci. 36 (1998) 1701–1739.
[2] A. Tuntomo, C.L. Tien, S.H. Park, Internal distribution of radiant absorption in a spherical particle, ASME J. Heat Transfer 113 (1991) 407–412.
[3] P.L.C. Lage, R.H. Rangel, Total thermal radiation absorption by a single spherical droplet, AIAA J. Thermophys. Heat Transfer 7 (1993) 101–109.
[4] D.W. Mackowski, R.A. Altenkirch, M.P. Menguc, Internal absorption cross sections in a stratified sphere, Appl. Opt. 29 (1990) 1551–1559.
[5] L.A. Dombrovsky, Thermal radiation from nonisothermal spherical particles of a semitransparent material, Int. J. Heat Mass Transfer 43 (2000) 1661–1672.
[6] M.F. Modest, Radiative Heat Transfer, McGraw-Hill, New York, 1993, pp. 61–64.